Genomic epidemiology of the rotavirus G2P[4] strains in coastal Kenya pre- and post-rotavirus vaccine introduction, 2012 – 2018

Timothy O. Makori [1, 2], Joel L. Bargul [2, 3], Arnold W. Lambisia [1], Mike J. Mwanga [1], Nickson Murunga [1], Zaydah R. de Laurent [1], Clement S. Lewa [1], Martin Mutunga [1], Paul Kellam[4, 5], Matthew Cotten [6,7], D. James Nokes [1, 8], My Phan[6, 7,*], and Charles N. Agoti [1, 9,*]

Affiliations:

1. Kenya Medical Research Institute (KEMRI)-Wellcome Trust Research Programme, off Hospital Road, Kilifi 80108, Kenya; tmakori@kemri-wellcome.org (T.O.M.); ALambisia@kemri-wellcome.org (A.W.L.); jmwanga@kemri-wellcome.org (M.J.M.); nmurunga@kemri-wellcome.org (N.M.); zdelaurent@gmail.com (Z.R.d.L.); CLewa@kemri-wellcome.org (C.L.); MMutunga@kemri-wellcome.org (M.M.); jnokes@kemri-wellcome.org (D.J.N.); cnyaigoti@kemri-wellcome.org (C.N.A.).
2. Department of Biochemistry, Jomo Kenyatta University of Agriculture and Technology, Juja 62000-00200, Kenya; Jbargul@jkuat.ac.ke (J.L.B).
3. International Centre of Insect Physiology and Ecology, Animal Health Theme, P.O. Box 30772-00100, Nairobi, Kenya; jbargul@icipe.org (J.L.B).
4. Department of Infectious Diseases, Fulculty of Medicine, Imperial College London, London, UK; p.kellam@imperial.ac.uk (P.K)
5. Kymab Ltd, The Bennet Building (B930), Babraham Research Campus, Cambridge, UK
6. Medical Research Centre (MRC)/ Uganda Virus Research Institute, Entebbe, Uganda
7. MRC-University of Glasgow, Centre for Virus Research Glasgow, United Kingdom; Matthew.Cotten@lshtm.ac.uk (M.C.); My.Phan@lshtm.ac.uk (MP).
8. School of Life Sciences and Zeeman Institute (SBIDER), The University of Warwick, Coventry CV4 7AL, UK
9. School of Health and Human Sciences, Pwani University, Kilifi 80108, Kenya

Keywords:
Rotavirus group A, G2P[4], Coastal Kenya

ABSTRACT

The introduction of rotavirus vaccines into the national immunization programme in many countries has led to a decline of childhood diarrhoea disease burden. Coincidentally, the incidence of some rotavirus group A (RVA) genotypes, has increased, which may result from non-vaccine-type replacement. Here we investigate the evolutionary genomics of rotavirus G2P[4] which has shown an increase in countries that introduced the monovalent Rotarix® vaccine. We examined the 63 RVA G2P[4] strains sampled from children (aged below 13 years) admitted to Kilifi County Hospital, Coastal Kenya, pre- (2012 to June 2014) and post- (July 2014-2018) rotavirus vaccine introduction. All the 63 genome sequences showed a typical DS-1 like genome constellation G2-P[4]-I2-R2-C2-M2-A2-N2-T2-E2-H2. G2 sub-lineage IVa-3 strains predominated in the pre-vaccine era co-circulating with low numbers of G2 sub-lineage IVa-1 strains, whereas sub-lineage IVa-3 strains dominated the post-vaccine period. In addition, in the pre-vaccine period, P[4] sub-lineage IVa strains co-circulated with low numbers of P[4] lineage II strains, but P[4] sub-lineage IVa strains predominated in the post-vaccine period. On the global phylogeny, the Kenyan pre- and post-vaccine G2P[4] strains clustered separately, suggesting that different virus populations circulated in the two periods. However, the strains from both periods exhibited conserved amino acid changes in the known antigenic epitopes, suggesting that replacement of the predominant G2P[4] cluster was unlikely a result of immune escape. Our findings demonstrate that the pre- and post-vaccine G2P[4] strains circulating in Kilifi, coastal Kenya, differed genetically, but likely were antigenically similar. This information informs the discussion on the consequences of rotavirus vaccination on rotavirus diversity.

INTRODUCTION

In 2009, the World Health Organization (WHO) recommended inclusion of rotavirus vaccines into the national immunization programmes (NIPs) globally [1]. Kenya introduced the WHO pre-qualified Rotarix® RVA (rotavirus group A) vaccine into its NIP in July 2014 [2]. With the increasing uptake of rotavirus vaccines globally, there has been a significant reduction in RVA-associated disease burden, but this virus still caused about 128,500 deaths in 2016 alone [3,4], with the majority of cases occurring in low-income countries [5]. In Kenya, post-vaccine introduction impact studies have reported significant reduction of rotavirus-associated diarrhoea hospitalization in children under five years, a vaccine effectiveness of ~64% [6], and a significant increase in the positivity rate of Rotarix® heterotypic genotypes such as G2P[4] and G3P[8] [7,8]. Similar findings were observed in other countries that introduced the Rotarix® vaccine in their NIPs [9–18]

Whole genome analysis of RVA can reveal the transmission and evolutionary history of circulating strains, including emerging mutations, and the origins and genetic diversity of the strains circulating in a particular region [19]. The rotavirus G2P[4] genotype is known to possess a DS-1 like genomic constellation (G2-P[4]-I2-R2-C2-M2-A2-N2-T2-E2-H2) [20]. G2P[4] strains are believed to have undergone genetic evolution in a stepwise pattern [21]. This is from lineage I to IVa in the NSP5, NSP1, VP2, VP4, and VP7 genome segments, and from lineage I to V in the VP1, VP3, VP6, NSP2, NSP3, and NSP4 genome segments, with some of the strains undergoing intragenotype reassortments in the VP7, VP3, and NSP4 genes after 2004 giving rise to emergent lineages of V in the VP7 segment, lineages VI and VII in the VP3 gene, and VI, VII, VIII, IX and X lineages in the NSP4 gene [21–23]. The G2P[4] lineages circulating in Kenya are unknown.

Characterization of South African G2P[4] strains, through comparison of strains occurring during pre-and post-introduction of Rotarix® vaccine, revealed sub-lineage shifts from G2 sub-lineage IVa-1 to G2 IVa-3, and P[4] sub-lineage IVa to P[4] IVb, and these shifts in genetic evolution were attributed to arise due to natural fluctuations and not as a result of vaccine pressure [24]. Similarly, G2P[4] whole genome analysis in Ghana [22], Australia [25,26], South Korea [11], Bangladesh [27], and Brazil [28] showed that implementation of Rotarix® vaccination does not influence genetic diversity of the circulating G2P[4] strains and common amino acid replacements in the VP7 antigenic epitopes including A87T, D96N, S213D were reported, irrespective of the vaccination period.

The main goal of this study was to conduct whole genome analysis of the G2P[4] genotypes circulating in Kilifi County, Kenya, to determine whether introduction of Rotarix® vaccine in Kenya's NIP impacts on the genetic diversity of the circulating G2P[4] viral populations. Data from this study were compared with contemporaneous global RVA strains to establish the phylogenetic context and potential origin of the Kenya's pre- and post-vaccination rotavirus G2P[4] strains.

MATERIALS AND METHODS

Ethical approval

We collected samples from children to screen for and determine the genetic diversity of rotavirus group A (RVA) viral populations. The study was conducted with strict adherence to the study protocols approved by the Scientific and Ethics Review Unit (REF: #3049 and #2861) at the Kenya Medical Research Institute, KEMRI, Nairobi, Kenya. Parents and guardians of the eligible children were provided with sufficient information about the research study to allow each individual to make informed and independent decisions for their children to be enrolled in the study. Sample collection proceeded after obtaining written informed consent from the parents and guardians.

Study participants

The study was based at Kilifi County Hospital (KCH), a referral health facility that mainly serves the people of Kilifi County located in the North Coast of Kenya [29]. Stool samples were obtained from children, aged below 13 years, who presented with diarrhoea as one of the illness symptoms and were admitted at KCH [6,30]. Diarrhoea was defined as passing of watery stool at least three times in the last 24 hours.

The stool samples were screened to detect RVA by using ELISA kit (ProSPect™; Oxoid, Basingstoke UK). All the RVA positive samples were initially genotyped by partial segment sequencing approach [7]. VP7 and VP4 genes were sequenced, and G and P genotypes inferred using the Virus Pathogen Resource (VIPR) tool for RVA [31]. Those classified as G2P[4] based on the outer capsid proteins were selected for this study (Fig. 1) [7].

RNA extraction and processing

The samples collected in the pre-vaccine period (January 2012 – June 2014) were sequenced using agnostic whole genome sequencing method [32], while the post-vaccine

samples (July 2014 – December 2018) were sequenced using an amplicon-based whole genome sequencing approach [33,34].

Processing of pre-vaccine samples was done by centrifugation of 110 µL of stool suspension in PBS (phosphate buffered saline) for 10 minutes at 10,000 × g. Next, 2 U/µl of TURBO DNase (#AM2238; Life Technologies, Carlsbad, USA) were added to degrade non-encapsulated DNA. Nucleic acid extraction was performed according to the Boom method [35]. First strand cDNA was synthesized using the SuperScript III Reverse Transcriptase Kit (#18064014; Life Technologies, Carlsbad, USA) with non-ribosomal random hexamer primers [36]. Second strand cDNA was synthesized using 5U of Klenow fragment 3' – 5' exo- (#M0212S; New England Biolabs, Ipswich, USA).

Processing of post-vaccine introduction samples was done by subjecting 200 mg of stool specimens to bead beating [37], followed by nucleic acid extraction using the QIAamp Fast DNA Stool Mini kit (#51604; Qiagen, Manchester, UK) following the manufacturer's instructions. Reverse Transcription-PCR (RT-PCR) was performed using the SuperScript IV One-Step RT-PCR System (#2594025, Thermo Fisher Scientific, Waltham, USA) following the manufacturer's instructions. The published primers used in our study to conduct RT-PCR assays were adopted from earlier studies (Table S1) [33,34]. The PCR conditions for the non-structural gene segments (NSP1, NSP2, NSP3, NSP4, and NSP5) consisted of 40 cycles of thermocycling (30 seconds at 90°C, one minute at 55°C, and four minutes at 68°C), whereas amplification of structural gene segments (VP1, VP2, VP3, VP4, VP6, and VP7) included 40 cycles of thermocycling (90°C for 30 seconds, 61°C for one minute and 68°C for six minutes), and included a final extension at 72°C for four minutes. PCR amplicons were resolved under a 2% agarose gel stained with RedSafe (iNtRON Biotechnology, Inc) for visualization of DNA bands. PCR products were purified using Exonuclease I (#EN0581; Thermo Fisher Scientific, Waltham, USA) as described by the manufacturer and pooled for each sample.

Next generation sequencing

Preparation of standard Illumina libraries for pre-vaccine samples was performed according to the published protocol [32]. Briefly, the double-stranded cDNA for each sample was sheared to obtain 400 – 500 nucleotide fragments. Each sample was then indexed separately to unique adapters and multiplexed at 95 samples and then sequenced on a HiSeq platform to generate about 1.5 million 250bp paired end reads per sample.

For the post-vaccine samples was done by purifying the pooled amplicons for each sample using the Agencourt AMPure XP Kit (#A63881; Beckman Coulter, USA) as described by the manufacturer. Library preparation was performed using the Illumina DNA flex (#20025519, Illumina, San Diego, USA) as per the manufacturer's specifications. Briefly, bead-linked transposomes were used to tagment the DNA, followed by addition of adapters to the DNA fragments using a limited PCR program. The adapter-linked DNA was cleaned using the tagment wash buffer. After that, the purified tagmented DNA was amplified via a limited-cycle PCR program that adds the i7, i5 adapters and sequences required for cluster generation during sequencing. Next, the amplified libraries were purified using a double-sided bead purification method. Subsequently, each DNA library was quantitated, and correct insert sizes confirmed on an Agilent 2100 Bioanalyzer using the Agilent high sensitivity DNA kit (#5067; Agilent, Santa Clara, USA). The DNA libraries were quantified on the Qubit fluorimeter 2.0 using the Qubit dsDNA HS Assay kit (#Q32851, Life Technologies, Thermo Fisher Scientific, Waltham, USA), normalized, and pooled at equimolar concentrations. Pooled DNA libraries were denatured and sequenced on the Illumina MiSeq platform (Illumina, San Diego, USA) to generate 150 paired end reads.

Genome assembly

Quality trimming of Illumina FASTQ reads was done using Trimmomatic (Phred score >30) with the following flags "ILLUMINACLIP: adapters_file: 2:30:10 LEADING:3 TRAILING:3 SLIDINGWINDOW: 4:15 MINLEN:36" to remove adapters and low-quality bases [38]. De-Novo assembly of the quality trimmed reads was done using Spades with the following flags "-k 99,127 --careful" [39]. For the pre-vaccine sequences, RVA-specific contigs were identified using USEARCH [40] and a SLIM algorithm [41]. Partial and overlapping contigs were joined using Sequencher [42] to obtain full-length sequences. For the post-vaccine sequences, Quast was used to check the quality of the contigs [43]. Next, artemis was employed to determine the ORFs of each RVA segment [44]. Then, genotyping of the assembled pre- and post-vaccine sequences was done using the Virus Pathogen Resource tool for RVA [31]. The nucleotide sequences generated in this study have been deposited into GenBank under accession numbers MZ093788 to MZ097268 and OP677569 to OP677754 (Table S2).

Global sequences collection and processing

All available G2P[4] sequences irrespective of the sequence length and their corresponding metadata, including year of collection and location were downloaded from the Virus Pathogen Resource of RVA [31]. Records missing metadata were manually searched

and any information, including location and collection year, that could be found in the primary publications was included in the respective sequence data. The sequences were subset to obtain datasets of each genome segment. The datasets of all the genome segments were filtered to only include samples with all the 11 segments. For all the 11 segments, more that 80 % of the coding sequence (CDS) region was considered for analysis. Overall, 350 global sequences for each segment met the inclusion criteria for phylogenetic analyses (Table S2).

Phylogenetic analysis

The global dataset was combined with the sequences of this study for each genome segment and aligned using MAFFT (v7.487) with the command "mafft --auto --reorder --preservecase input_file.fasta > output_file.fasta" [45]. Maximum likelihood phylogenetic trees were reconstructed using IQTREE2 (v2.1.3) [46] using the best model selection [47] and 1000 bootstrap replication settings [48]. The ML trees were linked to the respective metadata in R v4.1.0 and the "ggTree" R package used to plot and visualize the trees [45]. For lineage designation, sequences of previously described lineages for each segment [21–23] were utilized as the references (Table S2).

Statistical analyses

All statistical analyses were carried out using Stata v13.1 [49]. Chi-square test was used to compare among groups, with $P< 0.05$ indicating statistical significance.

RESULTS

Baseline characteristics of the study participants

Peaks of rotavirus A (RVA) infections coincided with cases of diarrhoea during the study period between May and September (Fig. 1). However, sample collection was majorly disrupted in 2016 and 2017 by strikes of health care providers (Fig. 1) [6]. One huge peak of G2P[4] infections was observed between June and November 2016 (post-vaccine) and a small one documented between May and September 2012 (pre-vaccine) (Fig. 1).

No significant difference was reported in age, age groups, gender, and vaccination status between the cases infected with G2P[4] genotypes and the non-G2P[4] genotypes ($P>0.05$) (Table 1). G2P[4] genotypes were detected in 87 samples (20.3%), of which 63 (14.7%) were successfully full-genome sequenced (Table 1). Of the sequenced samples, 13 (20.6%) were from children who received two doses of the Rotarix® vaccine (Table 1).

Genome constellations

To determine the genetic diversity in the Kilifi G2P[4] strains and their genetic relatedness with global strains, near full-genome sequences (>80% genome coverage) of 63 Kilifi samples were sequenced from the pre- (n=33) and the post- (n=30) vaccine periods (Table S2). Using the Virus Pathogen Resource (VIPR) for RVA genotype determination [31], all the 63 sequences were classified as G2-P[4]-I2-R2-C2-M1-A2-N2-T2-E2-H1 genotype (DS-1-like typical genome constellation) as shown in Table S3.

Phylogenetic and sequence analysis

To gain insights into the genetic diversity of the study G2P[4] strains in the global context, genetic distance-resolved phylogenetic trees were constructed for all the 11 gene segments (Fig. 2 & Fig. S1). Sequence identity matrices of the study G2P[4] strains exhibited high nucleotide sequence similarities (93 – 100%) in the NSP1, NSP2, NSP3, NSP5, VP1, VP2, VP4, VP6, and VP7 genome segments, and low to high nucleotide sequence similarity (85 – 100%) in the VP3 and NSP4 genes (Table 2).

Analysis of the VP7 gene

The VP7 gene is highly variable and encodes the humoral immune response glycoprotein [50]. The VP7 genetic distance-resolved phylogenetic tree showed that the Kilifi sequences formed three clusters: a monophyletic cluster, a minor monophyletic cluster, and a singleton (Fig. 2). Within the major cluster, the Kilifi strains separated by vaccination period, with one subcluster consisting of strains circulating two years after Rotarix® vaccine introduction and were interspersed with three strains isolated from children admitted to Kenyatta National Hospital (KNH), Kenya in 2017 (Fig. 2). These sequences shared two non-synonymous amino acid substitutions (S72G, S75L) with respect to the pre-vaccine strains (Table S4). The second subcluster mainly consisted of strains circulating in the pre-vaccine period and two strains that circulated in July 2014, i.e., early post-vaccine period (Fig. 2). The sequences in the minor monophyletic cluster consisted of five Kilifi strains collected in 2012, while the singleton Kilifi strain (KLF1033/2018) clustered with three strains detected in Mozambique in 2013 (Fig. 2).

With regards to the VP7 lineages, the Kilifi G2 strains were classified into lineage IV and further classified into sub-lineage IVa-1 and IVa-3 (Fig. 2). In 2012, sub-lineages IVa-1 and IVa-3 sequences co-circulated in Kilifi, while in the global context sub-lineages IVa-1, IVa-3 and IV non-a co-circulated (Fig. 3A). However, IVa-1 strains in Kilifi were replaced with sub-lineage IVa-3 strains in 2013 that dominated until 2018 (Fig. 3A), unlike in the global

context where sub-lineages IVa-1, IVa-3 and V co-circulated in 2013, sub-lineage IVa-1 predominantly circulated in 2014, IVa-1 and V co-circulated in 2015, and IVa-3 re-emerged in 2016 replacing lineage V and co-circulated with sub-lineage IVa-1 until 2018 (Fig. 3A). No lineage shift was observed pre- and post-vaccine introduction.

Analysis of the VP4 gene

The VP4 gene is highly variable and encodes a highly immunogenic protease sensitive protein involved in receptor binding and cell penetration [50]. In the VP4 phylogenetic tree, the P[4] Kilifi sequences formed clusters (n>2) mainly based on the vaccination period separated from global sequences (Fig. 2). However, two Kilifi sequences formed singletons, with the KLF1033/2018 strain clustering with a sequence isolated from a child admitted to KNH, while the KLF0616/2012 strain was interspersed with sequences from Mozambique (Fig. 2). A major cluster of Kilifi sequences further sub-clustered based on the vaccination period, with the post-vaccine sequences interspersing with Kenyan sequences isolated from children admitted to KNH (Fig. 2). In addition, Kilifi strains collected in 2014 and some 2012 strains formed two distinct clades, clustering separately from global sequences (Fig. 2).

During the study period, G2 lineages II and IVa strains circulated in Kilifi, with lineages II and IV co-circulating in 2012, consistent with the global context (Fig. 3B). From 2013 to 2018, sub-lineage IVa predominantly circulated in Kilifi similar the global context (Fig. 3B). However, in the global context, few lineage II strains co-circulated with IVa strains in 2017 (Fig. 3B). No lineage shift was observed pre- and post-vaccine introduction (Fig 2).

Analysis of the backbone genome segments

The backbone genome segments of the Kilifi G2P[4] strains (VP6, VP1-VP3, and NSP1-NSP5) formed up to four clusters on the global phylogenetic trees (Fig.S1). In the VP6, VP1, VP2, VP3, NSP1, and NSP2 genes, majority of the Kilifi sequences formed one major cluster which further separated into two sub-clusters of only pre- and post-vaccine sequences (Fig. S1). The post-vaccine strains in these genes clustered closely with 2017 sequences from KNH, Kenya (Fig.S1). In addition, the Kilifi 2014 sequences in the VP6, VP3, NSP1, and NSP2 segments exhibited a different clustering pattern of a further minor sub-cluster irrespective of the vaccination period, consistent with the VP4 gene (Fig. S1). Four post-vaccine sequences were interspersed with the pre-vaccine sequences in the NSP4 gene and a singleton of post-vaccine sequence clustered with pre-vaccine sequences in the NSP3 gene (Fig. S1). The NSP5 post-vaccine sequences formed one cluster, while the pre-vaccine

sequences exhibited a different clustering pattern consisting of three distinct clusters (n≥2) and three singletons (KLF0601/2012 was interspersed with a sequence from KNH, KLF1066/2014 and KLF0722/2014) (Fig. S1). A minor cluster consisting of five Kilifi pre-vaccine strains (KLF0550/2012, KLF0551/2012, KLF0553/2012, KLF0558/2012, and KLF1064/2012) separate from global sequences was observed in the VP1, VP2, VP3, NSP2, NSP4, and NSP5 genes; however, interspersed with sequences that circulated between 2012 and 2017 in Japan, Hungary, Australia, and Belgium in the NSP3 gene and further formed two sub-clades in the VP6 gene (Fig. S1). In addition, a minor cluster of Kilifi pre-vaccine sequences (KLF0640/2013, KLF0673/2013, and KLF0657/2013) interspersed with sequences from Malawi was observed in the VP3 gene, indicating possible importation of these strains (Fig. S1). Besides, a singleton of a post-vaccine sequence (KLF1033/2018) was interspersed with sequences from Mozambique that circulated in 2013 across all the backbone genes (Fig. S1). For the NSP5 gene, three other singletons were observed: KLF0601/2012 interspersed with a sequence from KNH, KLF1066/2014 and KLF0722/2014 each separate from global sequences (Fig. S1). No lineage shifts were reported in the backbone genome segments (Fig. S1).

Amino acid changes in the VP7 glycoprotein (G) and VP4 Protease sensitive (P) proteins

The pattern of amino acid (aa) substitutions in the G and P proteins was analysed in relation to the ancestral DS-1 sequence. The VP7 gene contains 7-1 (7-1a and 7-1b) and 7-2 antigenic epitopes, which affect the ability of antibodies to neutralize virus infectivity and reduce vaccine effectiveness [51]. The Kilifi strains exhibited 17 aa changes relative to the DS-1 VP7 ancestral sequence (Table S4). All the Kilifi strains had three aa mutations (D96N, N125T, and V129M) in the 7-1a antigenic epitope with respect to the DS-1 ancestral strain (Fig. 4 & Table S4). Furthermore, except for the 2014 sequences, the Kilifi sequences exhibited an A87T aa mutation in the 7-1a epitope (Table S4). Compared to the DS-1 sequence, the Kilifi sub-lineage IVa-1 strains exhibited the N242 aa mutation, whereas sub-lineage IVa-3 strains harboured the N213D aa mutation; both in the 71-b epitope. (Table S4). Besides, the I44M aa change was observed in the T lymphocyte epitope (40 – 52) of all the Kilifi strains (Table S4).

The VP4 surface protein is cleaved into the VP8* and the VP5* domains containing the 8-1 to 8-4 and 5-1 to 5-5 antigenic epitopes [52]. Analysis of the VP4 aa mutations revealed that the Kilifi strains differed only at three positions; Q114P or L114P and N133S in the 8-3

315 epitope and N89D in the 8-4 epitope, relative to the DS-1 prototype sequence (Fig 4 & Table
316 S5).

317 DISCUSSION

318 We investigated the evolutionary dynamics of G2P[4] strains sampled from children
319 admitted to Kilifi County Hospital, Coastal Kenya between 2012 and 2018. All the recovered
320 genomes showed a typical DS-1 like constellation consistent with findings from several
321 countries using the Rotarix® vaccine in their NIPs [21,22,24,53].

322 Separate clusters of pre- and post-vaccine sequences were observed in the VP1-VP4, VP6,
323 VP7, NSP1, NSP2, and NSP5 segments. However, the strains sampled in July 2014 (early
324 post-vaccine period) clustered with pre-vaccine strains across all the 11 gene segments in our
325 study possibly because the vaccine coverage was low and thus had no impact yet on the
326 circulating genotypes and lineages. Unique clusters of either G2P[4] or G1[P8] strains
327 separated by RVA vaccine period have been reported in South Africa [24], Rwanda [54],
328 Australia and Belgium [55], which were interpreting as reflecting natural genetic fluctuations
329 rather than vaccine induced evolution. However, the study NSP4 and NSP3 genes exhibited
330 some clusters of mixed pre- and post-vaccine sequences, indicating that in some strains the
331 pre-vaccine may have reassorted with post-vaccine introduction strains as similarly suspected
332 in Mozambique, albeit in G1P[8] [56].

333 Phylogenetic analyses indicated that the diversity of the Kilifi G2P[4] strains may have
334 been locally restricted both in the pre- and post-vaccine periods, since Kilifi sequences
335 clustered away from global sequences in all the 11 genome segments. In addition, limited
336 sequence data from Kenya and East Africa may have contributed to this uncertainty about the
337 regional context of Kilifi diversity. The Kilifi post-vaccine strains only clustered with
338 Kenyan sequences sampled from children admitted to Kenyatta National Hospital in 2017,
339 further suggesting locally restricted genetic evolution. However, one sample
340 (KLF1033/2018) consistently clustered with sequences from Mozambique and some pre-
341 vaccine strains were interspersed with global strains for the NSP3 segment, suggestive of
342 limited introduction from other countries. No lineage shift was observed pre- and post-
343 periods in Kilifi inconsistent with findings in South Africa [24] where RVA vaccine
344 introduction resulted in lineage shift. Furthermore, few G2 and P[4] lineages were in
345 circulation within Kilifi compared with the combined global data during the study period.

This supported our hypothesis that local drivers were responsible for the diversity within the Kilifi setting.

The Kilifi strains harbored six conserved amino acid (aa) substitutions in the VP7 antigenic epitopes; 7-1a and 7-1b with respect to the ancestral DS-1 G2P[4] strain. Three of these positions (A87T, D96N, and N213D) are critical for antibody binding and sequence changes here may lead to escape from host neutralizing antibodies [57]. The I44M aa change may affect cellular immunity as this region harbors a known T lymphocyte epitope (40-52) of the VP7 genes. All Kilifi strains had this change that potentially result in loss of recognition by T cells leading to escape from host immune responses [58,59]. Three aa acid changes were observed in VP4 antigenic epitopes in 8-4 (N89D) and 8-3 (Q114P or L114P and N133S) in the Kilifi strains. These have been associated with escape of attachment of the virus to host neutralizing monoclonal antibodies [60]. These aa substitutions were present in both pre- and post-vaccine Kilifi strains, suggesting they were not brought about by vaccine use.

This study had limitations. First, only sequences sampled from hospitalized children were analysed, thus may not conclusively reflect diversity that was in circulation in the entire coastal Kenya population. We only analysed a few genomes across the years. Second, we only recovered near complete genomes. Only 68% coverage was recovered in the VP4 segment.

In conclusion, our study reinforces the significance of genomic sequencing in monitoring the effect of vaccine pressure on circulating RVA strains in Kenya. The Kilifi strains to a large extent clustered based on the vaccination period and were separate from the global strains. Furthermore, conserved amino acid mutations were observed in the VP7 and VP4 antigenic epitopes of the pre- and post-vaccine strains, suggesting that the Rotarix® vaccine did not have a direct impact on the evolution of the circulating strains.

Data availability

The epidemiological data is available on the VEC dataverse (https://doi.org/10.7910/DVN/P4MRVF).

Funding information

This study was funded by the Wellcome Trust (102975, 203077). The authors Timothy Makori, and Charles Agoti were supported by the Initiative to Develop African Research Leaders (IDeAL) through the DELTAS Africa Initiative (DEL-15-003). The DELTAS Africa

Initiative is an independent funding scheme of the African Academy of Sciences (AAS)'s Alliance for Accelerating Excellence in Science in Africa (AESA) and supported by the New Partnership for Africa's Development Planning and Coordinating Agency (NEPAD Agency) with funding from the Wellcome Trust (107769/Z/10/Z) and the UK government. The views expressed in this publication are those of the authors and not necessarily those of AAS, NEPAD Agency, Wellcome Trust or the UK government.

Acknowledgement

We thank all the study participants for their contribution of study samples, their parents/guardians, members of the viral epidemiology and control research group (http://virec-group.org/) and colleagues at the KEMRI Wellcome Trust Research Programme for their useful discussions during the preparation of the manuscript. This paper is published with the permission of the Director of KEMRI.

Conflicts of interest

The authors declare no conflict of interest

References

1. WHO Rotavirus Vaccines. Rotavirus vaccines: WHO position paper - July 2021 [Internet]. 2021 [cited 2022 Aug 2]. Available from: https://www.who.int/publications/i/item/WHO-WER9628
2. Varghese T, Kang G, Steele AD. Understanding Rotavirus Vaccine Efficacy and Effectiveness in Countries with High Child Mortality. Vaccines (Basel) [Internet]. 2022 Mar 1 [cited 2022 Aug 2];10(3). Available from: /pmc/articles/PMC8948967/
3. Tate JE, Burton AH, Boschi-Pinto C, et al. Global, Regional, and National Estimates of Rotavirus Mortality in Children <5 Years of Age, 2000-2013. Clinical Infectious Diseases [Internet]. 2016 May 1 [cited 2020 Oct 20];62(suppl_2):S96–105. Available from: https://academic.oup.com/cid/article/62/suppl_2/S96/2478843
4. Troeger C, Khalil IA, Rao PC, et al. Rotavirus Vaccination and the Global Burden of Rotavirus Diarrhea among Children Younger Than 5 Years. JAMA Pediatr [Internet]. 2018 Oct 1 [cited 2020 Oct 20];172(10):958–65. Available from: https://jamanetwork.com/
5. Troeger C, Blacker BF, Khalil IA, et al. Estimates of the global, regional, and national morbidity, mortality, and aetiologies of diarrhoea in 195 countries: a systematic analysis for the Global Burden of Disease Study 2016. Lancet Infect Dis [Internet]. 2018 Nov 1 [cited 2020 Oct 20];18(11):1211–28. Available from: /pmc/articles/PMC6202444/?report=abstract
6. Khagayi S, Omore R, Otieno GP, et al. Effectiveness of Monovalent Rotavirus Vaccine Against Hospitalization With Acute Rotavirus Gastroenteritis in Kenyan Children. 2020 May 23 [cited 2020 Oct 26];70(11):2298–305. Available from: https://academic.oup.com/cid/article/70/11/2298/5536640
7. Mwanga MJ, Owor BE, Ochieng JB, et al. Rotavirus group A genotype circulation patterns across Kenya before and after nationwide vaccine introduction, 2010-2018. BMC Infect Dis [Internet]. 2020 Jul 13 [cited 2020 Oct 26];20(1):504. Available from: https://bmcinfectdis.biomedcentral.com/articles/10.1186/s12879-020-05230-0
8. Gikonyo JN u., Mbatia B, Okanya PW, Obiero GFO, Sang C, Steele D, Nyangao J. Post-vaccine rotavirus genotype distribution in Nairobi County, Kenya. International Journal of Infectious Diseases [Internet]. 2020 Nov 1 [cited 2022 Jun 12];100:434. Available from: /pmc/articles/PMC7670220/
9. Vizzi E, Piñeros OA, Oropeza MD, et al. Human rotavirus strains circulating in Venezuela after vaccine introduction: predominance of G2P[4] and reemergence of G1P[8]. Virol J [Internet]. 2017 Mar 21 [cited 2022 Aug 2];14(1):1–14. Available from: https://virologyj.biomedcentral.com/articles/10.1186/s12985-017-0721-9
10. Roczo-Farkas S, Kirkwood CD, Cowley D, et al. The Impact of Rotavirus Vaccines on Genotype Diversity: A Comprehensive Analysis of 2 Decades of Australian Surveillance Data. J Infect Dis [Internet]. 2018 Jul 13 [cited 2022 Aug 2];218(4):546–54. Available from: https://pubmed.ncbi.nlm.nih.gov/29790933/
11. Thanh HD, Tran VT, Lim I, Kim W. Emergence of Human G2P[4] Rotaviruses in the Post-vaccination Era in South Korea: Footprints of Multiple Interspecies Re-assortment Events. Scientific Reports 2018 8:1 [Internet]. 2018 Apr 16 [cited 2022 May 26];8(1):1–10. Available from: https://www.nature.com/articles/s41598-018-24511-y

12. Zeller M, Rahman M, Heylen E, et al. Rotavirus incidence and genotype distribution before and after national rotavirus vaccine introduction in Belgium. Vaccine [Internet]. 2010 Nov 3 [cited 2022 Aug 2];28(47):7507–13. Available from: https://pubmed.ncbi.nlm.nih.gov/20851085/
13. Khandoker N, Thongprachum A, Takanashi S, et al. Molecular epidemiology of rotavirus gastroenteritis in Japan during 2014-2015: Characterization of re-emerging G2P[4] after rotavirus vaccine introduction. J Med Virol [Internet]. 2018 Jun 1 [cited 2022 Aug 2];90(6):1040–6. Available from: https://pubmed.ncbi.nlm.nih.gov/29488230/
14. Carvalho-Costa FA, de Assis RMS, Fialho AM, et al. The evolving epidemiology of rotavirus A infection in Brazil a decade after the introduction of universal vaccination with Rotarix®. BMC Pediatr [Internet]. 2019 Jan 31 [cited 2022 Aug 2];19(1):1–10. Available from: https://bmcpediatr.biomedcentral.com/articles/10.1186/s12887-019-1415-9
15. Degiuseppe JI, Stupka JA. First assessment of all-cause acute diarrhoea and rotavirus-confirmed cases following massive vaccination in Argentina. Epidemiol Infect [Internet]. 2018 Nov 1 [cited 2022 Aug 2];146(15):1948. Available from: /pmc/articles/PMC6452988/
16. Simwaka JC, Mpabalwani EM, Seheri M, et al. Diversity of rotavirus strains circulating in children under five years of age who presented with acute gastroenteritis before and after rotavirus vaccine introduction, University Teaching Hospital, Lusaka, Zambia, 2008-2015. Vaccine [Internet]. 2018 Nov 12 [cited 2022 Aug 2];36(47):7243–7. Available from: https://pubmed.ncbi.nlm.nih.gov/29907481/
17. Al-Ayed MSZ, Asaad AM, Qureshi MA, Hawan AA. Epidemiology of group A rotavirus infection after the introduction of monovalent vaccine in the National Immunization Program of Saudi Arabia. J Med Virol [Internet]. 2017 Mar 1 [cited 2022 Aug 2];89(3):429–34. Available from: https://pubmed.ncbi.nlm.nih.gov/27531633/
18. Than VT, Jeong S, Kim W. A systematic review of genetic diversity of human rotavirus circulating in South Korea. Infect Genet Evol [Internet]. 2014 Dec [cited 2018 Mar 16];28:462–9. Available from: http://linkinghub.elsevier.com/retrieve/pii/S1567134814003086
19. Ghosh S, Kobayashi N. Whole-genomic analysis of rotavirus strains: Current status and future prospects [Internet]. Vol. 6, Future Microbiology. Future Medicine Ltd London, UK ; 2011 [cited 2020 Oct 26]. p. 1049–65. Available from: www.futuremedicine.com
20. Matthijnssens J, Ciarlet M, Rahman M, et al. Recommendations for the classification of group A rotaviruses using all 11 genomic RNA segments. Arch Virol [Internet]. 2008 [cited 2018 Jan 5];153(8):1621–9. Available from: http://link.springer.com/10.1007/s00705-008-0155-1
21. Doan YH, Nakagomi T, Agbemabiese CA, Nakagomi O. Changes in the distribution of lineage constellations of G2P[4] Rotavirus A strains detected in Japan over 32years (1980-2011). Infection, Genetics and Evolution [Internet]. 2015 Aug 1 [cited 2020 Oct 27];34:423–33. Available from: https://pubmed.ncbi.nlm.nih.gov/26026594/
22. Agbemabiese CA, Nakagomi T, Doan YH, Do LP, Damanka S, Armah GE, Nakagomi O. Genomic constellation and evolution of Ghanaian G2P[4] rotavirus strains from a global perspective. Infection, Genetics and Evolution. 2016 Nov 1;45:122–31.

23. Giammanco GM, Bonura F, Zeller M, et al. Evolution of DS-1-like human G2P[4] rotaviruses assessed by complete genome analyses. Journal of General Virology [Internet]. 2014 Jan 1 [cited 2020 Oct 27];95(PART 1):91–109. Available from: https://www.microbiologyresearch.org/content/journal/jgv/10.1099/vir.0.056788-0

24. Mwangi PN, Page NA, Seheri ML, et al. Evolutionary changes between pre- and post-vaccine South African group A G2P[4] rotavirus strains, 2003–2017. Microb Genom [Internet]. 2022 Apr 21 [cited 2022 May 26];8(4):000809. Available from: https://www.microbiologyresearch.org/content/journal/mgen/10.1099/mgen.0.000809

25. Donato CM, Pingault N, Demosthenous E, Roczo-farkas S, Bines JE. Characterisation of a G2P[4] Rotavirus Outbreak in Western Australia, Predominantly Impacting Aboriginal Children. Pathogens 2021, Vol 10, Page 350 [Internet]. 2021 Mar 16 [cited 2022 May 26];10(3):350. Available from: https://www.mdpi.com/2076-0817/10/3/350/htm

26. Donato CM, Zhang ZA, Donker NC, Kirkwood CD. Characterization of G2P[4] rotavirus strains associated with increased detection in Australian states using the RotaTeq® vaccine during the 2010-2011 surveillance period. Infect Genet Evol [Internet]. 2014 Dec 1 [cited 2018 Mar 16];28:398–412. Available from: http://linkinghub.elsevier.com/retrieve/pii/S1567134814001890

27. Aida S, Nahar S, Paul SK, et al. Whole genomic analysis of G2P[4] human Rotaviruses in Mymensingh, north-central Bangladesh. Heliyon. 2016 Sep 1;2(9):e00168.

28. Gómez MM, Carvalho-Costa FA, Volotão E de M, et al. Prevalence and genomic characterization of G2P[4] group A rotavirus strains during monovalent vaccine introduction in Brazil. Infect Genet Evol [Internet]. 2014 Dec [cited 2018 Mar 16];28:486–94. Available from: http://linkinghub.elsevier.com/retrieve/pii/S1567134814003402

29. Scott JAG, Bauni E, Moisi JC, et al. Profile: The Kilifi Health and Demographic Surveillance System (KHDSS). Int J Epidemiol [Internet]. 2012 Jun [cited 2022 Aug 3];41(3):650–7. Available from: https://pubmed.ncbi.nlm.nih.gov/22544844/

30. Otieno GP, Bottomley C, Khagayi S, et al. Impact of the introduction of rotavirus vaccine on hospital admissions for diarrhea among children in Kenya: A controlled interrupted time-series analysis. Clinical Infectious Diseases. 2020 Jun 1;70(11):2306–13.

31. Pickett BE, Sadat EL, Zhang Y, et al. ViPR: an open bioinformatics database and analysis resource for virology research. Nucleic Acids Res [Internet]. 2012 Jan [cited 2021 Oct 27];40(Database issue):D593. Available from: /pmc/articles/PMC3245011/

32. Phan MVT, Anh PH, Cuong N van, et al. Unbiased whole-genome deep sequencing of human and porcine stool samples reveals circulation of multiple groups of rotaviruses and a putative zoonotic infection. Virus Evol [Internet]. 2016 Jul [cited 2018 Mar 16];2(2):vew027. Available from: https://academic.oup.com/ve/article-lookup/doi/10.1093/ve/vew027

33. Fujii Y, Shimoike T, Takagi H, Murakami K, Todaka-Takai R, Park Y, Katayama K. Amplification of all 11 RNA segments of group A rotaviruses

based on reverse transcription polymerase chain reaction. Microbiol Immunol. 2012 Sep;56(9):630–8.

34. Magagula NB, Esona MD, Nyaga MM, et al. Whole Genome Analyses of G1P[8] Rotavirus Strains From Vaccinated and Non-Vaccinated South African Children Presenting With Diarrhea HHS Public Access. J Med Virol. 2015;87(1):79–101.
35. Boom R, Sol CJ, Salimans MM, Jansen CL, Dillen PMW, Noordaa J van der. Rapid and simple method for purification of nucleic acids. J Clin Microbiol [Internet]. 1990 [cited 2021 Oct 27];28(3):495. Available from: /pmc/articles/PMC269651/?report=abstract
36. Endoh D, Mizutani T, Kirisawa R, et al. Species-independent detection of RNA virus by representational difference analysis using non-ribosomal hexanucleotides for reverse transcription. Nucleic Acids Res [Internet]. 2005 [cited 2022 Aug 3];33(6):e65. Available from: /pmc/articles/PMC1074749/
37. Liu J, Gratz J, Amour C, et al. Optimization of quantitative PCR methods for enteropathogen detection. PLoS One. 2016 Jun 1;11(6).
38. Bolger AM, Lohse M, Usadel B. Trimmomatic: a flexible trimmer for Illumina sequence data. Bioinformatics [Internet]. 2014 Aug 1 [cited 2021 Oct 27];30(15):2114. Available from: /pmc/articles/PMC4103590/
39. Bankevich A, Nurk S, Antipov D, et al. SPAdes: A New Genome Assembly Algorithm and Its Applications to Single-Cell Sequencing. Journal of Computational Biology [Internet]. 2012 May 1 [cited 2018 Jan 5];19(5). Available from: http://www.ncbi.nlm.nih.gov/pubmed/22506599
40. USEARCH algorithm [Internet]. [cited 2022 Sep 28]. Available from: https://www.drive5.com/usearch/manual/usearch_algo.html
41. Cotten M, Oude Munnink B, Canuti M, Deijs M, Watson SJ, Kellam P, van der Hoek L. Full Genome Virus Detection in Fecal Samples Using Sensitive Nucleic Acid Preparation, Deep Sequencing, and a Novel Iterative Sequence Classification Algorithm. PLoS One [Internet]. 2014 Apr 2 [cited 2022 Sep 28];9(4):e93269. Available from: https://journals.plos.org/plosone/article?id=10.1371/journal.pone.0093269
42. Sequencher DNA Sequence Analysis Software from Gene Codes Corporation [Internet]. [cited 2022 Sep 28]. Available from: http://www.genecodes.com/
43. Gurevich A, Saveliev V, Vyahhi N, Tesler G. QUAST: quality assessment tool for genome assemblies. Bioinformatics [Internet]. 2013 Apr 15 [cited 2021 Oct 27];29(8):1072. Available from: /pmc/articles/PMC3624806/
44. Carver T, Harris SR, Berriman M, Parkhill J, McQuillan JA. Artemis: an integrated platform for visualization and analysis of high-throughput sequence-based experimental data. Bioinformatics [Internet]. 2012 Feb [cited 2021 Oct 27];28(4):464. Available from: /pmc/articles/PMC3278759/
45. Katoh K, Misawa K, Kuma K, Miyata T. MAFFT: a novel method for rapid multiple sequence alignment based on fast Fourier transform. Nucleic Acids Res [Internet]. 2002 Jul 15 [cited 2021 Oct 28];30(14):3059. Available from: /pmc/articles/PMC135756/
46. Minh BQ, Schmidt HA, Chernomor O, Schrempf D, Woodhams MD, von Haeseler A, Lanfear R. IQ-TREE 2: New Models and Efficient Methods for Phylogenetic Inference in the Genomic Era. Mol Biol Evol [Internet]. 2020 May 1 [cited 2021 Oct 28];37(5):1530–4. Available from: https://academic.oup.com/mbe/article/37/5/1530/5721363

47. Subha K, Minh BQ, Wong TKF, von Haeseler A, Jermiin LS. ModelFinder: Fast model selection for accurate phylogenetic estimates. Nat Methods. 2017 May 30;14(6):587–9.
48. Hoang DT, Chernomor O, Haeseler A von, Minh BQ, Vinh LS. UFBoot2: Improving the Ultrafast Bootstrap Approximation. Mol Biol Evol [Internet]. 2018 Feb 1 [cited 2021 Oct 28];35(2):518. Available from: /pmc/articles/PMC5850222/
49. Statistical software for data science | Stata [Internet]. [cited 2022 Oct 13]. Available from: https://www.stata.com/
50. Liu L. Fields Virology, 6th Edition. Clinical Infectious Diseases [Internet]. 2014 Aug 15 [cited 2022 Sep 15];59(4):613–613. Available from: https://academic.oup.com/cid/article/59/4/613/2895607
51. Aoki ST, Settembre EC, Trask SD, Greenberg HB, Harrison SC, Dormitzer PR. Structure of rotavirus outer-layer protein VP7 bound with a neutralizing Fab. Science [Internet]. 2009 Jun 6 [cited 2022 Aug 11];324(5933):1444. Available from: /pmc/articles/PMC2995306/
52. Dormitzer PR, Sun ZYJ, Wagner G, Harrison SC. The rhesus rotavirus VP4 sialic acid binding domain has a galectin fold with a novel carbohydrate binding site. EMBO Journal. 2002 Mar 1;21(5):885–97.
53. Dennis AF, McDonald SM, Payne DC, et al. Molecular epidemiology of contemporary G2P[4] human rotaviruses cocirculating in a single U.S. community: footprints of a globally transitioning genotype. J Virol [Internet]. 2014 Apr 1 [cited 2018 Mar 15];88(7):3789–801. Available from: http://jvi.asm.org/cgi/doi/10.1128/JVI.03516-13
54. Rasebotsa S, Mwangi PN, Mogotsi MT, et al. Whole genome and in-silico analyses of G1P[8] rotavirus strains from pre- and post-vaccination periods in Rwanda. Scientific Reports 2020 10:1 [Internet]. 2020 Aug 10 [cited 2022 Aug 15];10(1):1–22. Available from: https://www.nature.com/articles/s41598-020-69973-1
55. Zeller M, Donato C, Trovão NS, et al. Genome-Wide Evolutionary Analyses of G1P[8] Strains Isolated Before and After Rotavirus Vaccine Introduction. Genome Biol Evol [Internet]. 2015 Sep 1 [cited 2022 Aug 15];7(9):2473–83. Available from: https://pubmed.ncbi.nlm.nih.gov/26254487/
56. Munlela B, João ED, Donato CM, et al. Whole Genome Characterization and Evolutionary Analysis of G1P[8] Rotavirus A Strains during the Pre- and Post-Vaccine Periods in Mozambique (2012–2017). Pathogens [Internet]. 2020 Dec 1 [cited 2022 Aug 19];9(12):1–19. Available from: /pmc/articles/PMC7762294/
57. Dyall-Smith ML, Lazdins I, Tregear GW, Holmes IH. Location of the major antigenic sites involved in rotavirus serotype-specific neutralization. Proc Natl Acad Sci U S A [Internet]. 1986 [cited 2022 Jun 3];83(10):3465–8. Available from: https://pubmed.ncbi.nlm.nih.gov/2422651/
58. Morozova O v., Sashina TA, Fomina SG, Novikova NA. Comparative characteristics of the VP7 and VP4 antigenic epitopes of the rotaviruses circulating in Russia (Nizhny Novgorod) and the Rotarix and RotaTeq vaccines. Arch Virol. 2015 Jul 15;160(7):1693–703.
59. Wei J, Li J, Zhang X, Tang Y, Wang J, Wu Y. A naturally processed epitope on rotavirus VP7 glycoprotein recognized by HLA-A2.1-restricted cytotoxic CD8+ T cells. Viral Immunol. 2009 Jun 1;22(3):189–94.
60. Monnier N, Higo-Moriguchi K, Sun Z-YJ, Prasad BVV, Taniguchi K, Dormitzer PR. High-Resolution Molecular and Antigen Structure of the VP8*

642 Core of a Sialic Acid-Independent Human Rotavirus Strain. J Virol [Internet].
643 2006 Feb [cited 2022 Aug 17];80(3):1513. Available from:
644 /pmc/articles/PMC1346936/
645
646
647

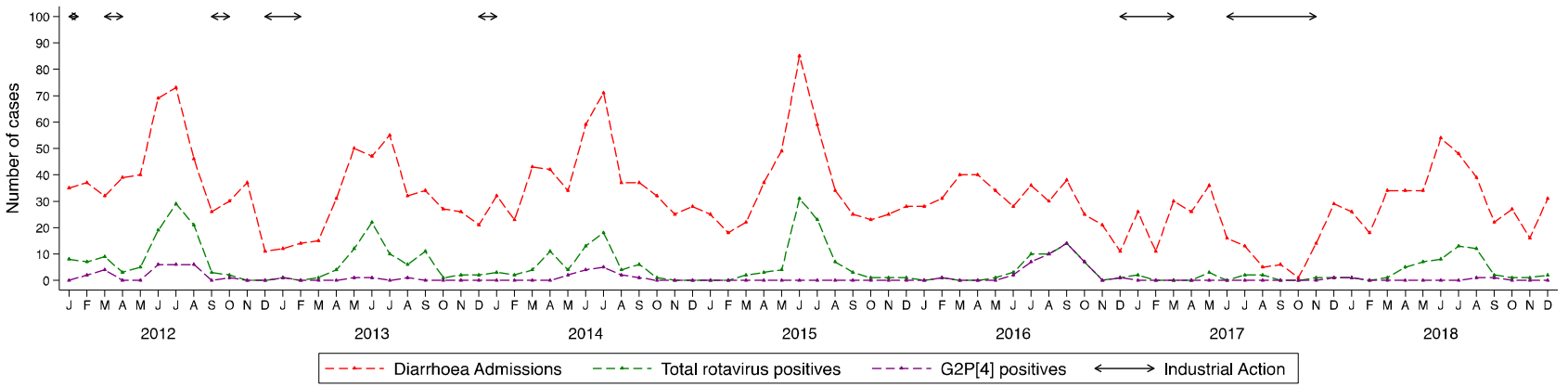

the G and P genotypes was by partial segment sequencing using the Sanger approach [7].

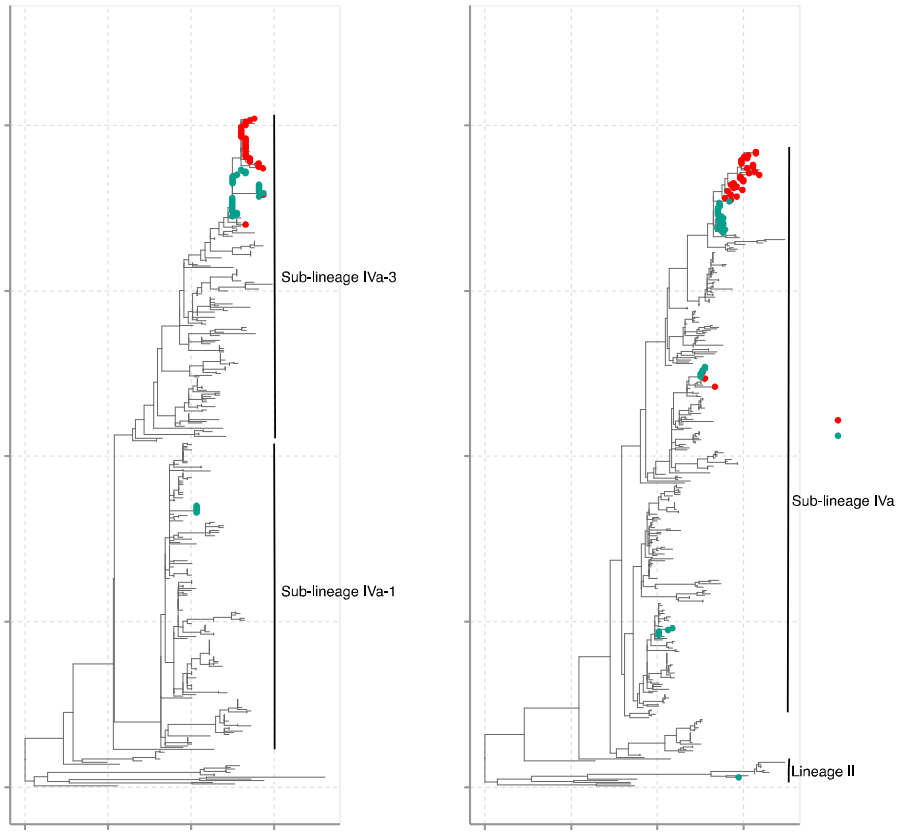

Fig. 2: Phylogenetic reconstruction of the 63 Kilifi G2P[4] sequences against a backdrop of 350 global sequences for the VP7 and VP4 RVA genome segments using maximum likelihood (ML) methods. The Kilifi sequences are colored by the period of sample collection (either before or after vaccine introduction in Kenya). For all the global sequences, more than 80% of the coding sequence (CDS) region was considered for analysis. For the Kilifi sequences, >80% CDS were used for the VP7 and 68% for the VP4 segment. The study sequences classified to the lineages indicated in each phylogenetic tree.

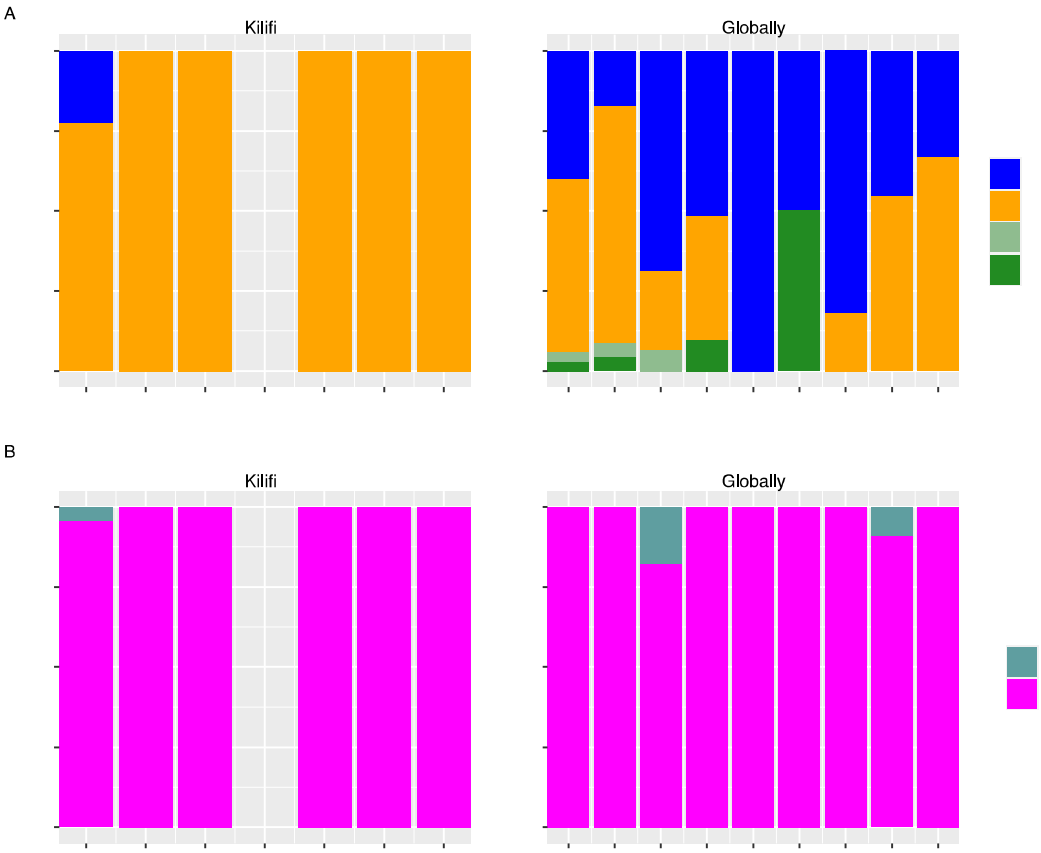

Fig. 3: Temporal pattern of the G2 and P[4] lineages observed in Kilifi and globally. (A) Temporal pattern of the Kilifi G2 lineages from 2012 to 2018 and temporal pattern of the global G2 lineages from 2010 to 2018. (C) Temporal pattern of the Kilifi P[4] lineages from 2012 to 2018 and temporal pattern of the global P[4] lineages from 2010 to 2018.

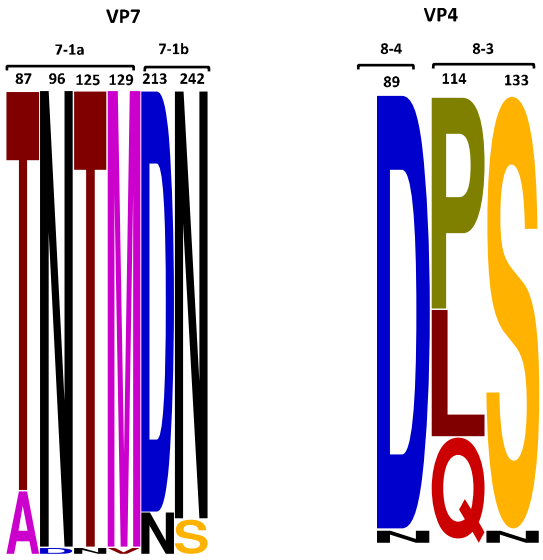

Fig. 4: A sequence logo showing the amino changes observed in known antigenic epitopes of G2 and P[4] proteins in the Kilifi G2P[4] relative to the ancestral DS-1 strain. The changes in amino acids are shown in different color schemes.

693 Supplementary Figure Legend

694 Fig. S1: Phylogenetic reconstruction of the 63 Kilifi G2P[4] sequences against a backdrop of
695 350 global sequences for the VP6, VP1, VP2, VP3, NSP1, NSP2, NSP3, NSP4, and NSP5
696 RVA genome segments using maximum likelihood (ML) methods. The Kilifi sequences are
697 colored by the period of sample collection (either before or after vaccine introduction in
698 Kenya). For the Kilifi and all the global sequences, more than 80% of the coding sequence
699 (CDS) region was considered for analysis. The study sequences classified to the lineages
700 indicated in each phylogenetic tree.

Table 1: Baseline demographic characteristics of the children that were rotavirus positive and those found to be G2P[4] infected during the study period (2012 to 2018)

Characteristics	RVA Positives (%)	Successfully Sequenced G2P[4] (%)	All G2P[4] (%)	non-G2P [4] (%)	All G2P[4] vs non-G2P[4] P-value
Total cases	429	63 (14.7)	87 (20.3)	342 (79.7)	
Vaccine period					0.039
Pre-vaccine	215 (49.9)	33 (52.4)	35 (40.2)	180 (52.6)	
Post-vaccine	214 (50.1)	30 (47.6)	52 (59.8)	162 (47.4)	
Age (in months)					0.944
Mean (SD)	14.9 (13.1)	17.6 (16.4)	16.9 (15.4)	14.4 (12.4)	
Median (IQR)	11.7 (8.3-17.9)	11.2 (8.6-20.7)	10.6 (8.4-19.7)	12.2 (8.3-16.8)	
Age group (in months)					0.092
0-11m	216 (50.4)	33 (52.4)	47 (54.0)	216 (50.4)	
12– 23m	169 (39.4)	20 (31.2)	26 (29.9)	143 (41.8)	
24– 59m	35 (8.2)	7 (11.1)	11 (12.6)	24 (7.0)	
>=60 m	9 (2.1)	3 (4.8)	3 (3.5)	6 (1.7)	
Gender					0.789
Male	251 (51.5)	37 (58.7)	52 (59.7)	199 (58.2)	
Vaccination status					0.129
Vaccinated	88 (20.6)	14 (22.2)	22 (25.6)	66 (19.4)	
Not vaccinated	215 (50.4)	33 (52.4)	35 (40.7)	180 (52.8)	
Unknown	124 (29.0)	16 (25.4)	29 (33.7)	95 (27.9)	
[1]Full vaccination	79 (18.4)	13 (20.6)	21 (24.1)	58 (17.0)	0.256

[1] Full vaccination implies that the participants received two doses of the Rotarix vaccine as recommended by WHO

Table 2: Percentage nucleotide and amino acid identity for the Kilifi G2P[4] strains

Genome segment	Percentage nucleotide similarity	Percentage amino acid similarity
VP4	94.3-100	96.8-100
VP7	94.3-100	96.3-100
VP6	94.0-100	96.0-100
VP1	93.9-100	98.0-100
VP2	97.2-100	99.2-100
VP3	87.1-100	92.1-100
NSP1	95.7-100	96.0-100
NSP2	97.3-100	97.5-100
NSP3	97.1-100	98.4-100
NSP4	85.0-100	91.5-100
NSP5	94.5-100	94.5-100